Stereoscopic study of the angle-dependent magnetoresistance oscillations across the charge-density-wave transition of the organic conductor α-(BEDT-TTF)$_2$KHg(SCN)$_4$

W. Kang*
Department of Physics, Ewha Womans University, Seoul 120-750, Korea

T. Osada, T. Konoike, and K. Uchida
Institute for Solid State Physics, University of Tokyo, Kashiwa, Chiba 277-8581, Japan

(Received 23 June 2013; revised manuscript received 9 September 2013; published 4 November 2013)

The stereoscopic angle-dependent magnetoresistance oscillations (AMRO) in an organic conductor α-(BEDT-TTF)$_2$KHg(SCN)$_4$ were measured across the temperature-pressure boundary that separates the charge-density-wave state from the metallic state. The gnomonic projections of the data clearly resolved the contributions from different parts of the Fermi surfaces. The temperature and pressure dependencies of the AMRO results revealed the progressive formation of a quasi-one-dimensional orbit in the charge-density-wave state. The AMRO measurements at ambient pressures and at low temperatures revealed the presence of two sets of quasi-one-dimensional Fermi surfaces. Additional evidence for multiple quasi-one-dimensional orbits was obtained from the data collected in conjunction with the in-plane field rotations.

DOI: 10.1103/PhysRevB.88.195105 PACS number(s): 71.18.+y, 71.45.Lr, 72.80.Le, 72.15.Gd

I. INTRODUCTION

The layered organic conductor α-(BEDT-TTF)$_2$KHg(SCN)$_4$, where BEDT-TTF denotes bis(ethylenedithio)tetrathiafulvalene, has been extensively investigated over the years.[1–9] At a pressure of 1 bar, this conductor undergoes a phase transition to a charge-density-wave (CDW) phase at a temperature T_{CDW} ($\sim$8 K).[10] T_{CDW} decreases with increasing pressure and vanishes above P_c (3–4 kbar).[11,12] The metallic electrical conductivity is preserved below T_{CDW}, and superconductivity is observed both below and above P_c.[12] The unusual properties revealed by this material over varying temperatures, pressures, and magnetic fields are closely related to the peculiar Fermi surfaces (FSs) of the materials, which consist of a pair of quasi-one-dimensional (Q1D) sheets that are open along the k_z direction and a closed quasi-two-dimensional (Q2D) cylindrical FS at the corners of the in-plane first Brillouin zone at room temperature (see the inset of Fig. 1).[13,14] The CDW is thought to originate from the nesting structure of the sheetlike FSs. The wave vector of the CDW, **Q**, is incommensurate with the crystal lattice and is tilted with respect to the conducting plane.[10]

Numerous angle-dependent magnetoresistance oscillations (AMRO) studies of α-(BEDT-TTF)$_2$KHg(SCN)$_4$ have been conducted, both at ambient pressures[4,6,7,9,15–17] and under hydrostatic pressures.[9] At 1 bar and at $T \ll T_{\mathrm{CDW}}$, the AMRO measurements are typical of Q1D FSs oriented 20°–30° away from the arrangement suggested by band calculations.[13] On the other hand, AMRO measurements collected from a metallic state ($T > T_{\mathrm{CDW}}$, $P > P_c$) correspond to the Q1D FSs obtained from the band calculations.[9,18] The Q2D FS AMRO signals coexist at strong magnetic fields above the kink transition[16] or above the CDW transition temperature at 1 bar.[17]

The AMRO signals at intermediate pressures and temperatures have been largely unexplored.[19] Similarly, the interplay between the CDW and superconductivity below P_c has not yet been characterized. The azimuthal dependence of the magnetoresistance during the rotation of the magnetic field in the plane parallel to the conducting layer warrants examination.

In certain samples in which multiple FSs produce complex AMRO patterns, stereoscopic studies that cover the full 4π solid angle offer powerful tools for resolving the different types of AMRO signals.[20,21] Using these techniques, we recently showed that the AMRO signals of a metallic phase coexisted with the AMRO signals of the CDW phase at low temperatures, and changed continuously at high temperatures immediately below T_{CDW}.[17] These effects were attributed to magnetic breakdown through the gaps formed on the cylindrical FS by the CDW potential. The experimental results could be reproduced in a quantum mechanical model without assuming a specific FS configuration.[17]

In this paper, we report fully stereographic AMRO measurements of the interlayer magnetoresistance in α-(BEDT-TTF)$_2$KHg(SCN)$_4$ over a wide range of pressures and temperatures across the CDW phase transition. In the metallic state, the Q1D and Q2D AMRO signals were found to coexist, consistent with the calculated band structures. The gnomonic projections of the stereographic AMRO data revealed previously unknown properties of the CDW state. The superposed complex AMRO signals at low pressures could be resolved into *two* clear sets of Q1D AMRO states. The weaker signal was nearly a mirror image of the principal Q1D AMRO signal with respect to the conducting layer plane, as observed previously in the sister compound α-(BEDT-TTF)$_2$RbHg(SCN)$_4$.[22] At intermediate pressures ($0 < P < P_c$) and well below T_{CDW}, the AMRO signals could be described as a mixture of the CDW phase and the original Q2D FS. The rotation of the magnetic field inside the conduction plane produced several dips in the magnetoresistance that could be explained by the formation of multiple Q1D orbits due to scattering by the incommensurate CDW potential.

II. EXPERIMENTS

Single crystals of α-(BEDT-TTF)$_2$KHg(SCN)$_4$ were grown using conventional electrochemical methods. Typical crystals

were relatively thick and were approximately rectangular in shape, with dimensions of $0.6 \times 0.5 \times 0.2$ mm^3. Electrical contacts between samples and 20-μm annealed gold wires were made using carbon paste. The interlayer resistance was measured along the crystallographic b^* axis using the standard four-probe technique. An ac current of the order of 10 μA was applied across the sample, and the voltages were measured using lock-in amplifiers. The pressure was varied by placing the sample in a miniature BeCu pressure cell at room temperature and pressing the cell using a hydraulic press. Between measurements, the pressure cell was warmed to room temperature to permit the pressure to change hydrostatically. Daphne 7373 oil was used as the pressure transmitting medium.[23] The precise value of the pressure at low temperatures was determined from the shift in the superconductivity transition temperature of a pure tin (Sn) element embedded adjacent to the sample under zero magnetic field conditions.[24] AMRO measurements were obtained at five different pressures: 1 bar, and 1.3, 1.9, 2.5, and 5.6 kbar. A double-axis rotator probe was used to rotate the pressure cell in a 14-T solenoid-type superconductor magnet. Throughout the experiments, the angles were set with respect to the pressure cell. Slight misorientations of the samples with respect to the pressure cell were numerically corrected by transforming the axes.

Measurements of the angle-dependent oscillations in the magnetoresistance provide a standard means for investigating the Fermi surfaces in layered conductors. Semiclassical calculations[6,25] based on the Boltzmann transport equation and quantum mechanical calculations based on interlayer electron tunneling[17] have successfully reproduced, at least qualitatively, most experimental observations. The magnetoresistance of a corrugated cylindrical FS displays a series of maxima for cases in which the magnetic field is tilted with respect to the cylinder axis. The positions of the maxima are periodic in $\tan\theta$ when the tilt angle θ is measured from the cylinder axis [Kartsovnik-Kajita-Yamaji (KKY) oscillations].[26–28] On the other hand, the magnetoresistance of a warped sheetlike FS displays a series of dips for cases in which the field is rotated around the normal axis of the Fermi sheet (Lebed resonances).[29–31] Additional modulations in the magnetoresistance have been reported for cases in which the magnetic field is rotated nearly coincidentally with the normal axis of the FS sheets [Danner-Kang-Chaikin (DKC) oscillations[32] and the third-angle effects[33,34]].

The AMRO behavior permitted the samples in this study to be classified as clean samples.[35]

III. RESULTS

Figure 1 summarizes the AMRO results $R_{zz}(\theta,\phi)$ obtained at four different pressures in the equirectangular projection. The azimuthal angle ϕ was measured relative to the crystallographic a axis, which corresponds to the 1D axis of the normal metallic phase. Four different types of AMRO signal were compared here: Shubnikov–de Haas (SdH) oscillations, KKY resonances, and Lebed resonances in the metallic and CDW states.

The data obtained from the normal metallic phase ($P = 5.6$ kbar, $T = 1.5$ K) clearly differed from the data obtained from the CDW phase ($P = 1$ bar, $T = 1.5$ K). Whereas the dominant feature of the AMRO in the CDW state was a series of Lebed resonances, similar to those presented in Ref. 17, the AMRO signals in the metallic state consisted of a superposition of the KKY oscillations (bright wavy curves) and the much sharper Lebed resonances (dark and sharp lines). The Lebed resonances at 1 bar and at 5.6 kbar differed in many respects: (1) the number of resonances in the CDW phase was larger than the corresponding number in the metallic phase; (2) the oscillation period was smaller in the metallic state; (3) the resonances were sharper and narrower in the metallic state; (4) the resonance convergence points (the direction of the relevant Q1D FS) differed by $\sim 23^\circ$. A detailed analysis is provided in the following.

Increasing the pressure while holding the temperature constant at 1.5 K clearly demonstrated how the AMRO signals evolved during the transition from the CDW state to the metallic state. The AMRO signal at 1.3 kbar was nearly indistinguishable from the signal obtained at 1 bar; however, a slightly higher pressure of 1.9 kbar produced substantial differences. Increases in the pressure and temperature produced approximately the same effects by weakening the CDW amplitude. The AMRO signal obtained at 1.9 kbar and at 1.5 K resembled those obtained at 1.3 kbar and at 4.5 K. The dramatic changes in the AMRO signal at higher pressures could be clearly observed by stereoscopically plotting the angle-dependent conductivity $\ln\sigma_{zz}(\theta,\phi)$ (lower panel of Fig. 1).

The temperature dependence of the AMRO signal at intermediate pressures clearly revealed the evolution of the AMRO signals from the CDW state to the metallic state. For example, the data collected at 1.3 kbar shows that the AMRO signal at 1.5 K was nearly identical to the signal obtained at 1 bar; however, the signals obtained above 5.5 K were closer to the signal obtained at 5.6 kbar and 1.5 K. Both the high-pressure Lebed resonances and the KKY resonances gradually appeared as the temperature was increased beyond 3.5 K. Around 4.5 K, the three resonances (the CDW state Lebed resonance, the KKY resonance, and the metallic state Lebed resonances) were superimposed, as observed at 1.9 kbar and at 1.5 K.

The fourth oscillations, SdH oscillations, also existed near $\theta = 0^\circ$ and 180° at all pressures. These oscillations could not be distinguished in Fig. 1 because their amplitudes were much smaller than those of the other oscillations; however, an enlarged view of the gnomonic projection of $R_{zz}(\theta,\phi)$ at $P = 5.6$ kbar, $T = 1.5$ K, and $H = 14$ T around the $\theta = 0$ direction (Fig. 2) clearly revealed the superposition of the SdH oscillations over the KKY resonances and the Lebed resonances. The frequency of these oscillations, which was proportional to the area of the Q2D FS, increased superlinearly with the pressure ($H_0 = 685.9 + 10.20P + 1.148P^2$) and was 14% larger at 5.6 kbar than at 1 bar.[9,36,37] A small additional oscillation with frequency of 894 T was observed at 2.5 kbar. These oscillations could correspond to the 850-T oscillations at 1 bar reported in Refs. 18 and 19. The amplitude of these oscillations did not follow the Lifshitz-Kosevich formula.

All AMRO oscillations present in the metallic state penetrated the CDW state through all parts of the P-T boundary

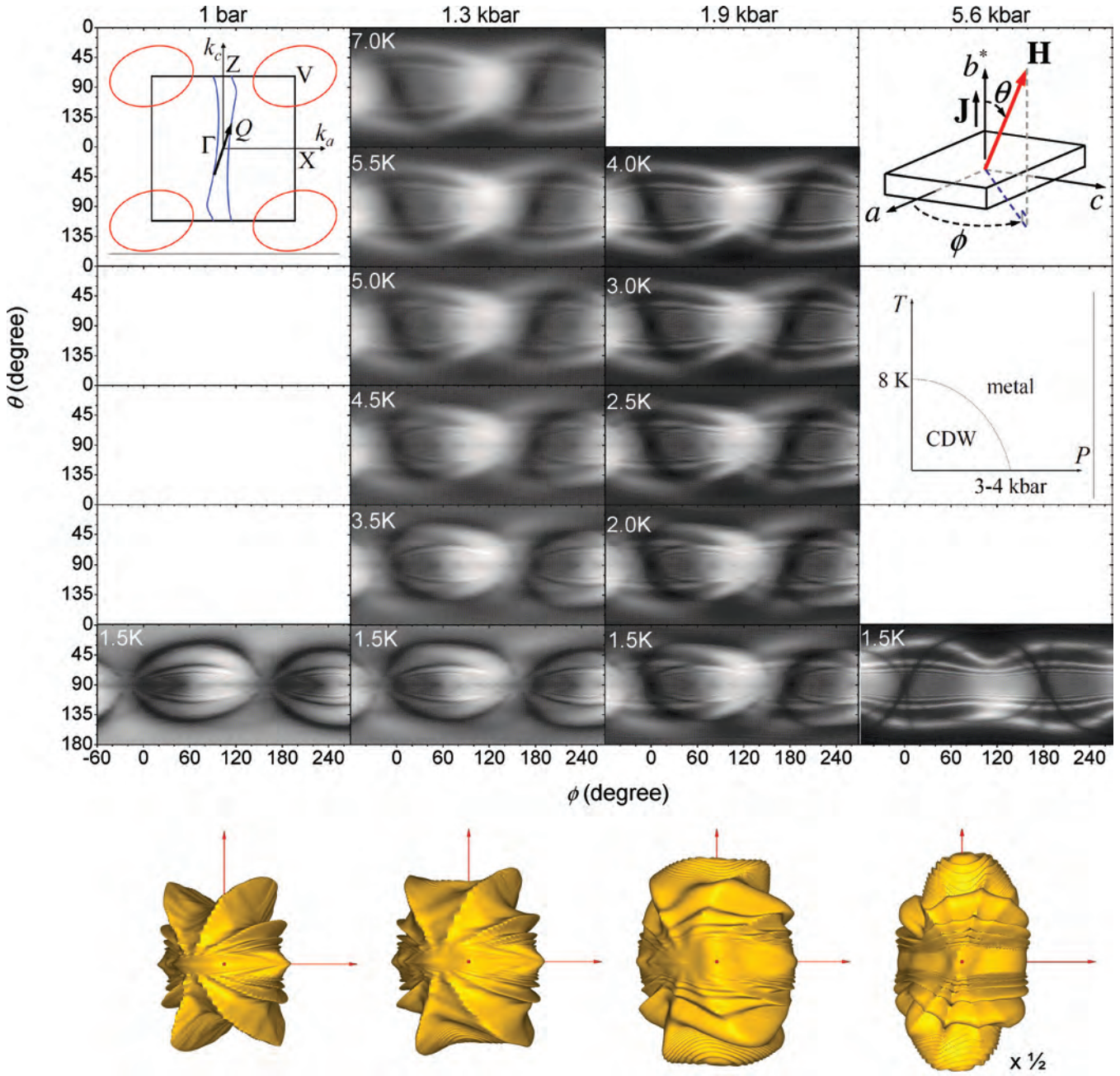

FIG. 1. (Color online) Pressure and temperature dependencies of the interlayer magnetoresistance $R_{zz}(\theta,\phi)$ at four different pressures, in the equirectangular projection. The brightness at a given position is proportional to the resistance value upon application of a magnetic field of fixed strength 14 T along that direction. The darkness scale differs from panel to panel. In some panels, the full 4π solid angle was not measured, but was completed for comparison by assuming inversion symmetry. Clockwise from the top left, the insets show schematic diagrams of the Fermi surfaces in α-(BEDT-TTF)$_2$KHg(SCN)$_4$ based on the calculations conducted by Mori *et al.*[13] and Harrison *et al.*,[14] the sample geometry and the definition of angles used in the text, and a temperature-pressure phase diagram, respectively. The cartoon below each column shows a three-dimensional plot of $\ln\sigma_{zz}(\theta,\phi)$ at 1.5 K, as seen from the crystallographic a axis.

between two states. By contrast, the low-temperature and low-pressure Lebed resonances were observed only inside the CDW state surrounded by the P-T boundary.

IV. DISCUSSION

The interpretation of the various AMRO signals becomes straightforward when the magnetoresistance is presented as a density plot in the gnomonic projection about the direction normal to conducting planes ($\theta = 0$). This projection is equivalent to a polar coordinate projection with $\tan\theta$ as the radial distance and ϕ as the angle. Three representative AMRO signals displayed simple geometric traces in this projection: (1) the SdH oscillations appeared as closely but *not* equally spaced concentric circles; (2) the KKY resonances appeared as equally spaced circles or, more often, as ellipses because of the in-plane anisotropy; and (3) the Lebed resonances appeared as straight lines parallel to the one-dimensional axis.

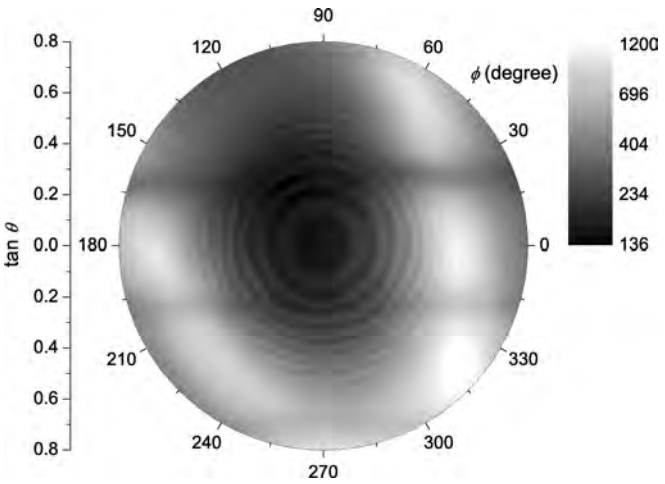

FIG. 2. Enlarged view of the gnomonic projection of $R_{zz}(\theta,\phi)$ at $P = 5.6$ kbar, $T = 1.5$ K, and $H = 14$ T around the $\theta = 0$ direction. Three principal oscillations corresponding to the metallic state are present: the broad white curves indicate the KKY resonances, dark horizontal traces indicate the Lebed resonances, and the closely placed concentric rings indicate the SdH oscillations.

We begin with a comparison of the representative data from the metallic and the CDW states. The left column in Fig. 3 shows the AMRO of the metallic state ($H = 14$ T, $P = 5.6$ kbar, and $T = 1.5$ K) in the equirectangular and gnomonic projections. Three different families of oscillations were present and were superposed. The data may be more readily interpreted from the gnomonic than from the equirectangular representation [Fig. 3(b)]. The direction and spacing between the clearly resolved black horizontal lines (0.49 in $\tan\theta \sin\phi$) agreed well with the Lebed resonances expected from the crystal structure[13] and with previously reported results.[9] The current stereoscopic study clearly revealed that the resonance lines were sharp and were resolved up to very large values of $\tan\theta \cos\phi$ [Fig. 3(b)], although the number of distinguishable resonance lines was the same as the number reported in Ref. 9. A series of large obliquely elongated rings corresponded to the KKY oscillations. The elongated nature of these rings reflected asymmetry in the conducting plane. The major axis of the ellipse was obliquely elongated by 110° from the 1D axis, in qualitative agreement with the Q2D FS calculated from the band structure.[13,14] Both the KKY oscillations and the conventional SdH oscillations (Fig. 2) were expected from the closed Q2D FS.

Despite the presence of clear Lebed resonances, related phenomena, such as DKC oscillations and third-angle effects, were not observed at all. This situation resembled that observed in the Q1D conductor $(TMTSF)_2ReO_4$, in which

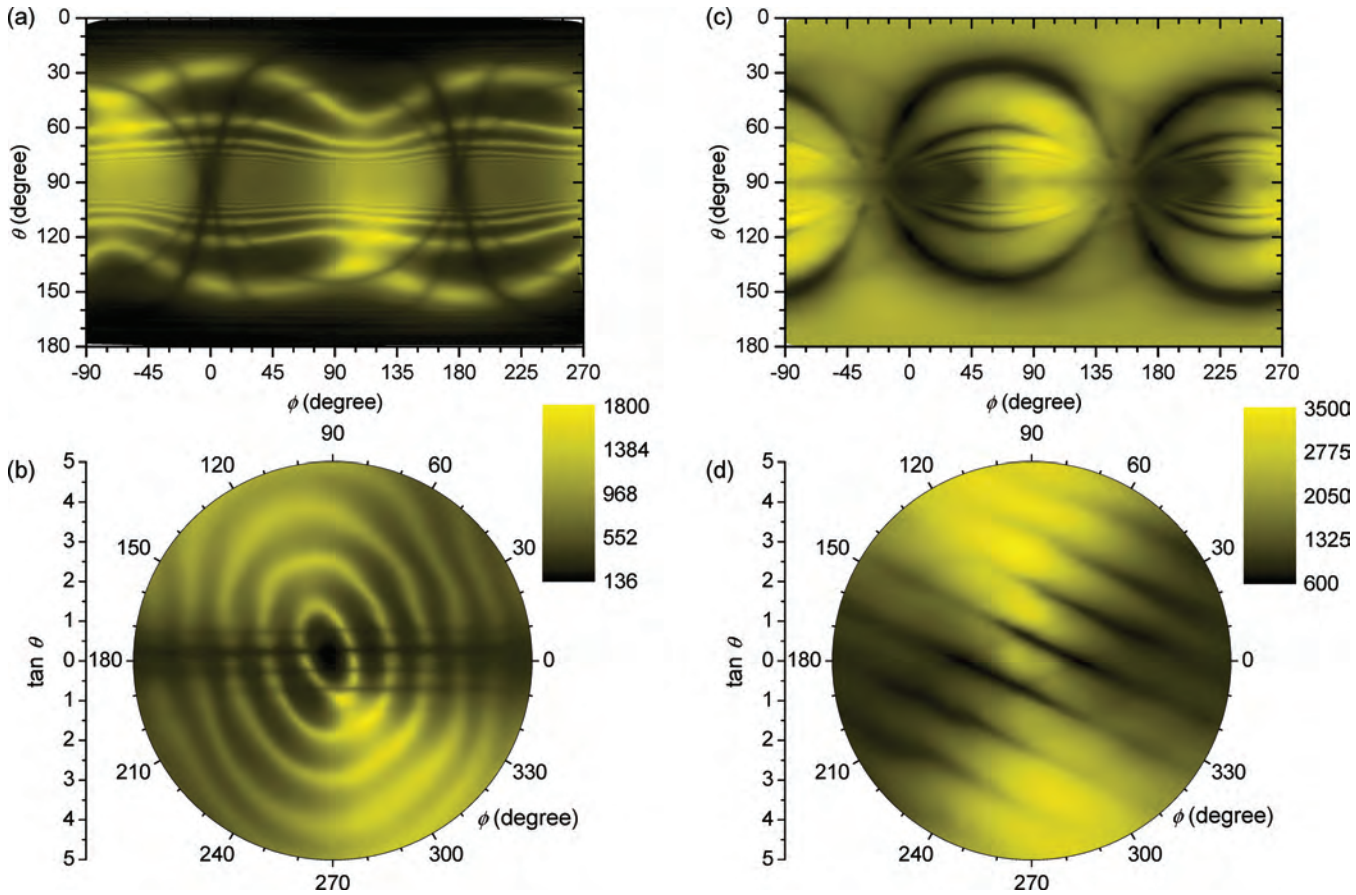

FIG. 3. (Color online) Comparison of the AMRO signals $R_{zz}(\theta,\phi)$ obtained from the metallic state (left column, $P = 5.6$ kbar) and the CDW state (right column, $P = 1$ bar). The top row shows the AMRO signals in the equirectangular projection and the bottom row shows the same signals in the gnomonic projection. In the gnomonic projections, the elliptical bright lines indicate the KKY resonances and the black lines indicate the Lebed resonances. $H = 14$ T and $T = 1.5$ K.

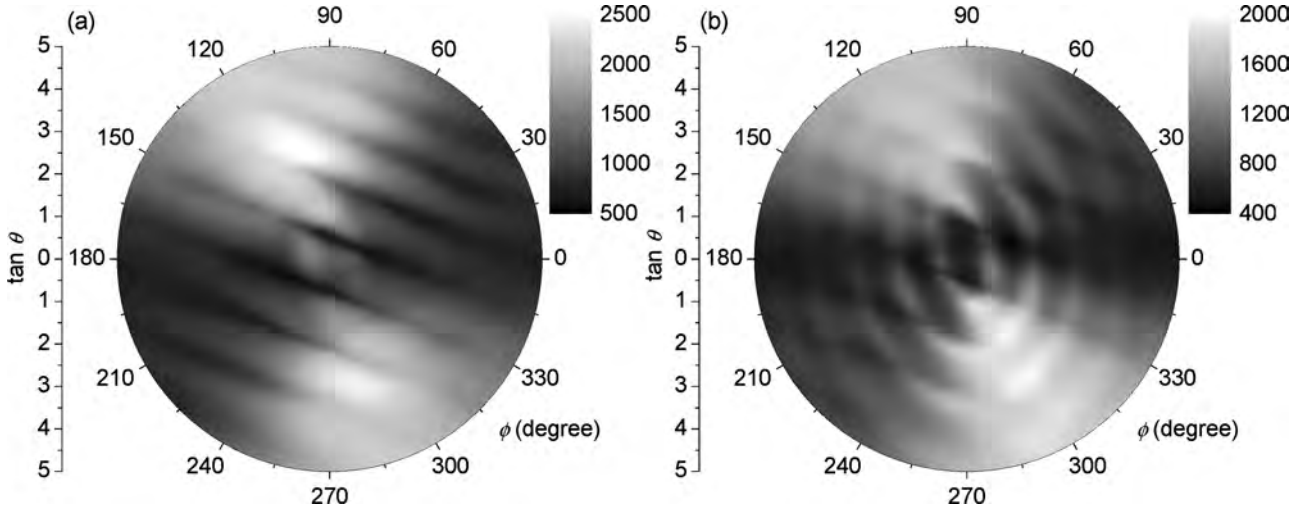

FIG. 4. Gnomonic projections of the AMRO signal $R_{zz}(\theta,\phi)$ at two intermediate pressures, (a) 1.3 kbar and (b) 2.5 kbar, show progressive changes within the CDW phase. $H = 14$ T and $T = 1.5$ K.

commensurate anion ordering was present in samples in which Lebed resonances were observed; however, in the present case of $P > P_c$ for α-(BEDT-TTF)$_2$KHg(SCN)$_4$, contributions from the Q1D and Q2D FSs were well separated and additive. The absence of third-angle effects may result from the relatively large contributions of the Q2D FS, which can

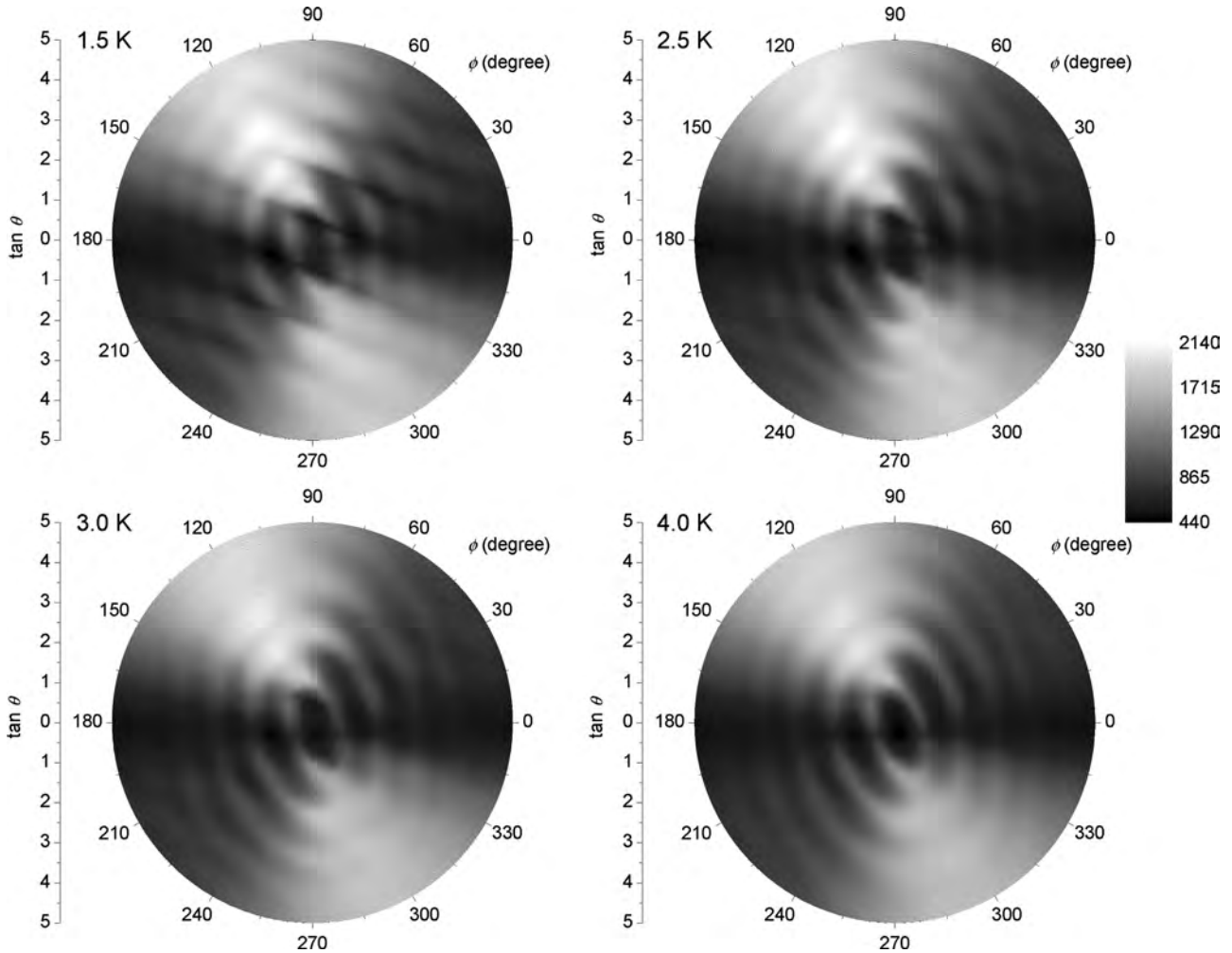

FIG. 5. The temperature dependence of the AMRO signal $R_{zz}(\theta,\phi)$ at $P = 1.9$ kbar and $H = 14$ T shows the progressive changes both within the CDW phase and across the phase boundary.

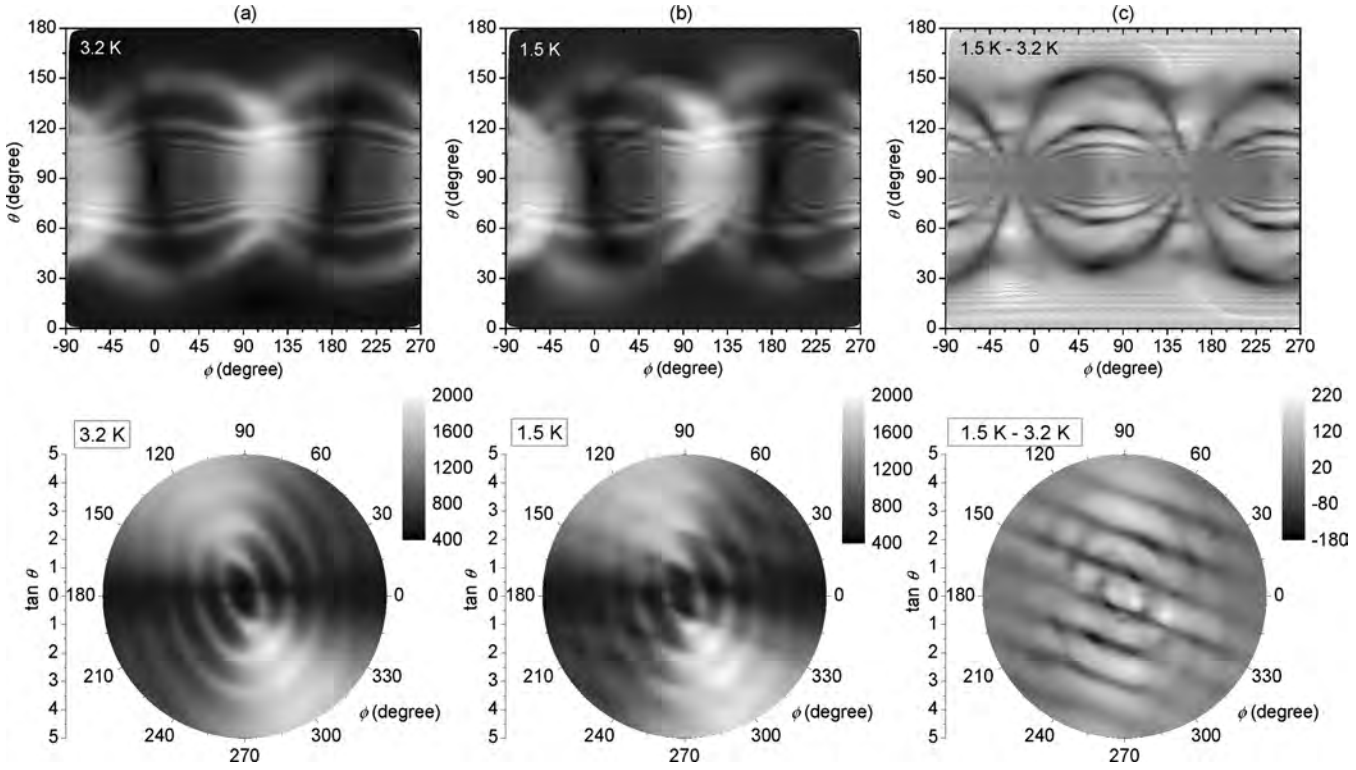

FIG. 6. Comparison of the AMRO signals obtained between $T > T_{CDW}$ and $T < T_{CDW}$, at a pressure of 2.51 kbar, in the equirectangular (upper row) and gnomonic (lower row) representations. The third column lists the difference between the resistance values at the two temperatures, obtained by numerically subtracting the 3.2-K data from the 1.5-K data.

obscure such effects. The absence of DKC oscillations could not be readily understood only in terms of the presence of the Q2D FS.

The data collected at ambient pressures are presented in the equirectangular and gnomonic projections in the right-hand column of Fig. 3. The origin of the azimuthal direction is the same as that shown in the left-hand column. In this case, the sample was deep in the CDW state, and the Q1D FS of the metallic state was believed to be completely suppressed by the CDW transition, although the temperature dependence of the electrical resistance remained metallic. Previous stereographic measurements of the interlayer magnetoconductivity, performed at 2 K and at 1 bar, reported anomalous Lebed resonance oscillations with an amplitude that appeared to have been modulated, as in the case of the DKC oscillations, over a broad range of azimuthal angles.[17] Apart from its unusually large width, the broad diamondlike pattern initially appeared to resemble the pattern typical of a Q1D system, such as are observed in TMTSF compounds.[20]

Presenting the data in the gnomonic projection revealed interesting features that could not be distinguished from the equirectangular projections [Fig. 3(d)]. Both the horizontal Lebed resonances and the KKY resonances from the Q2D FS were absent. Instead, a new series of Lebed resonances, with a period of $\tan\theta$ equal to two and a half times the period obtained from the metallic state, were present along a direction tilted 23° relative to the previous angle. Both the direction and the period of the new set of Lebed resonances suggested that these signals arose from a set of Q1D FSs that was distinct from those present in the metallic state.[38] Several groups have reported similar results for the CDW state.[4–9,16,17]

Strikingly, the gnomonic projection revealed a weaker second set of Lebed resonances at the mirrored positions of the primary Lebed resonances about the k_x axis ($\phi = 0$). All fuzzy structures present in the equirectangular projection, which were previously attributed to the DKC oscillations and the third-angle effects,[17] were in fact merged into a new set of Lebed resonances as observed previously in the sister compound α-(BEDT-TTF)$_2$RbHg(SCN)$_4$.[22] The period of these resonances was similar to that of the principal Lebed resonances (1.275 versus 1.258, respectively). Although we can not completely rule out the possibility of sample twinning without performing x-ray experiments on the same crystal used for the current study, a more plausible scenario is that multiple nesting vectors $\boldsymbol{Q} = \pm \boldsymbol{Q}_a + \boldsymbol{Q}_c$ were present, as suggested by Kovalev *et al.*[8,22] Although one vector would be dominant in the absence of a magnetic field, a strong magnetic field would restrict the electron motion to a trajectory perpendicular to the field while favoring motion in the other directions.

The AMRO signals collected at intermediated pressures, 1.3 and 2.5 kbar, are shown in the gnomonic projection in Fig. 4. The data collected at 1.3 kbar resemble those collected at 1 bar, with the exception of two features: the secondary Lebed resonances were almost negligible, and the KKY resonances had begun to develop from the center. The change was even clearer at 2.5 kbar: the primary Lebed resonance remained dominant, and no traces of the secondary Lebed resonance were observed. The KKY resonances, however, were well

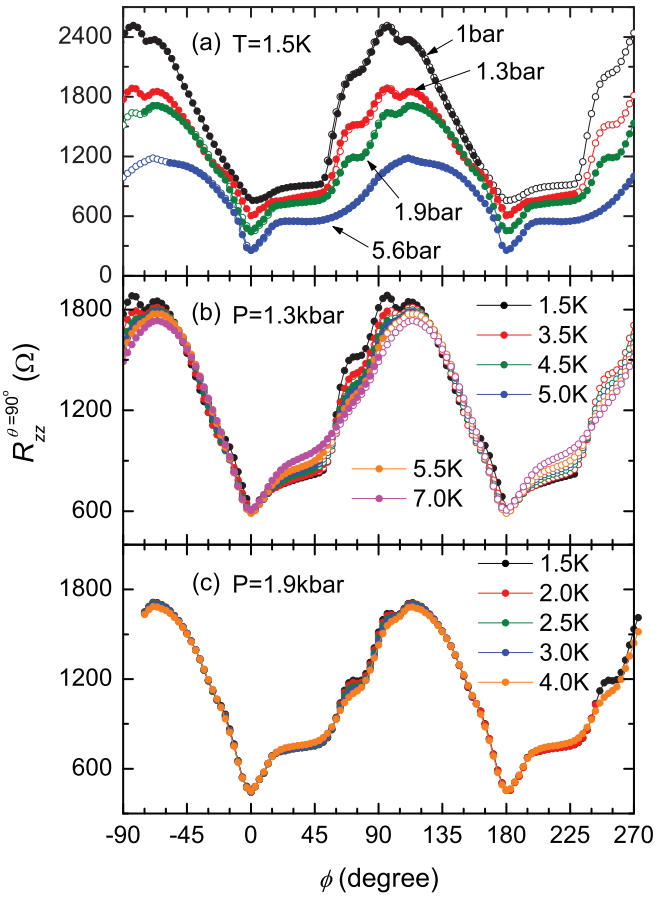

FIG. 7. (Color online) Pressure and temperature dependence of the interlayer magnetoresistance $R_{zz}(90^\circ,\phi)$ for the case in which the magnetic field is exactly aligned with the conducting layers. All curves displayed a sharp minimum at $\phi = 0^\circ$ and 180°, corresponding to the 1D axis of the metallic state. The open symbols plot the data represented by the black symbols, except that the data are shifted by 180° to facilitate a comparison.

developed at this pressure. The presence of the tilted Lebed resonance clearly indicated that a pressure of 2.5 kbar fell below P_c at $T = 1.5$ K. The presence of a broad faint horizontal pattern suggested that the metallic 1D FS had begun to reestablish itself at this pressure. Near the CDW phase boundary, a part of the original Q1D FS appeared to survive, even after CDW nesting, because the CDW gap remained too small to completely remove the Q1D FS. These observations collectively suggest that the reconstructed Q1D FS coexisted with the Q2D FS.[38] The reconstructed Q1D FS could not be structurally resolved, although it was effectively formed by magnetic breakdown.

The CDW could be suppressed by increasing the hydrostatic pressure, and an increase in the temperature was found to provide the same result. Figure 5 shows the temperature dependence of the AMRO signal in the gnomonic projection at $P = 1.9$ kbar. This pressure was clearly below P_c at 1.5 K. Lebed resonances from the reconstructed Q1D Fermi surface were well developed at 1.5 K and gradually disappeared as the temperature was increased beyond 3 K. By contrast, the KKY resonances were omnipresent over the whole temperature range, suggesting that the original Q2D FS was relevant everywhere in the phase diagram. Broad and dark horizontal lines suggested that the original Q1D FS was present throughout the temperature range. At 4 K, the original Q1D FS was fully restored, but the Lebed lines were not sharp due to temperature broadening.

The analysis discussed thus far has revealed that the original Q1D FS of the metallic state was gradually suppressed during entry into the CDW state, and a new species of Q1D FS formed as the CDW scattering potential increased.[38] It should be noted that all three FSs coexisted over a wide swath of the P-T phase diagram. Figure 6 illustrates this observation directly. The AMRO signals were measured at 3.2 and 1.5 K at 2.5 kbar. The temperatures were, respectively, above (or very close to) and below T_{CDW} at this pressure.[39] Both the equirectangular and the gnomonic projections agreed with the observations described above. An interesting feature was revealed by subtracting the data collected at 3.2 K from that collected at 1.5 K. This process corresponded to removing the contributions of the metallic state FSs from the low-temperature data. The results represent the contribution of the reconstructed CDW FS alone and are nearly indistinguishable from the data obtained at 1.5 K and 1 bar.

The detailed stereoscopic study also determined the interlayer resistance under a magnetic field rotating in the conducting plane. Figure 7 shows $R_{zz}(\theta = 90^\circ,\phi)$ for various pressures and temperatures. A pronounced minimum was observed under conditions in which the magnetic field was oriented along the crystallographic a axis, regardless of the sample state (CDW or metallic). No trace of the third-angle effects was observed in the metallic or reconstructed Q1D FS. The absence of third-angle effects may be closely related to the absence of DKC oscillations. It should be noted that the signal features did not change upon increasing either the temperature or the pressure. These results suggested that the Q2D FS in the metallic state was progressively reconstructed by the superlattice potential upon entering into the CDW phase.

Additional dips were observed in the signals obtained from the CDW state. These features corresponded to dark spots along the $\theta = 90^\circ$ line in Fig. 3(c). Such dips have not been observed in any other system. The presence of additional dips may result from the additional Q1D orbits formed by the incommensurate CDW scattering potential. Subjecting Q2D FSs of reasonable size (16% of the FBZ in the current system) to the periodic potential exerted by the CDW will simultaneously induce connections of all Q2D FSs via reciprocal lattice vectors. More than one Q1D orbit is then possible. The positions of the dips roughly correspond to the directions estimated from the known nesting vector $\boldsymbol{Q}$. Some of these directions may not be as efficient as others in generating Lebed resonances, although they may be sufficiently efficient to create a resistance dip under conditions in which the magnetic field is perpendicularly aligned.

V. CONCLUSIONS

We isolated the AMRO resonances from the metallic and CDW states using full stereographic techniques. As a sample enters a CDW state from the metallic state, during either a decrease in the temperature or pressure, the stereographic AMRO patterns gradually change from those characteristic

of a metallic state to those characteristic of a CDW state. The metallic state AMRO patterns did not clearly indicate the boundary separating the CDW phase from the metallic phase. The AMRO patterns of the metallic phase ($T > T_{CDW}$ and $P > P_c$) coexisted with those of the CDW phase ($T < T_{CDW}$ and $P < P_c$) over a broad range of conditions that favor the crystallographically defined CDW phase. This observation strongly supports the assertion that an increase in the amplitude of a CDW periodic potential affects the electron motion in the metallic state Q2D FS. Both Q1D and Q2D behaviors are then possible through Bragg reflections and magnetic breakdown. The former is dominant deep in the CDW phase, but the latter is dominant close to the phase boundary. We showed that the two effects could be resolved numerically. Complex Q1D-like AMRO signals deep inside the CDW state could be reduced to a pair of Lebed resonances without DKC oscillations. The scattering by the CDW potential is expected to create more complex electron trajectories than previously anticipated.

ACKNOWLEDGMENTS

The authors thank K. Kobayashi and M. Saito for growing single crystals. This work was supported by a grant from the National Research Foundation of Korea (NRF), funded by the Korean Government (MSIP) (Grants No. 2011-0030902, No. 2010-00453, and No. 2008-0061893), and by a Grant-in-Aid for Scientific Research (KAKENHI) on Innovative Areas from MEXT of Japan (Grant No. 23110705).

*wkang@ewha.ac.kr

[1] M. V. Kartsovnik, in *The Physics of Organic Superconductors and Conductors*, edited by A. G. Lebed (Springer, Berlin, 2008), pp. 185–246; S. Uji and J. S. Brooks, in *The Physics of Organic Superconductors and Conductors*, edited by A. G. Lebed (Springer, Berlin, 2008), pp. 89–126.

[2] J. Singleton, Rep. Prog. Phys. **63**, 1111 (2000); J. Wosnitza, *Fermi Surfaces of Low-Dimensional Organic Metals and Superconductors* (Springer, Berlin, 1996); T. Ishiguro, K. Yamaji, and G. Saito, *Organic Superconductors*, 2nd ed. (Springer, Berlin, 1998); A. A. House, S. J. Blundell, M. M. Honold, J. Singleton, J. A. A. J. Perenboom, W. Hayes, M. Kurmoo, and P. Day, J. Phys.: Condens. Matter **8**, 8829 (1996).

[3] M. Oshima, H. Mori, G. Saito, and K. Oshima, Chem. Lett. **18**, 1159 (1989).

[4] T. Osada, R. Yagi, A. Kawasumi, S. Kagoshima, N. Miura, M. Oshima, and G. Saito, Phys. Rev. B **41**, 5428 (1990).

[5] M. V. Kartsovnik, V. N. Laukhin, S. I. Pesotskii, I. F. Schegolev, and V. M. Yakovenko, J. Phys. I **2**, 89 (1992).

[6] Y. Iye, R. Yagi, N. Hanasaki, S. Kagoshima, H. Mori, H. Fujimoto, and G. Saito, J. Phys. Soc. Jpn. **63**, 674 (1994).

[7] T. Sasaki and N. Toyota, Phys. Rev. B **49**, 10120 (1994).

[8] A. E. Kovalev, M. V. Kartsovnik, R. P. Shibaeva, L. P. Rozenberg, I. F. Schegolev, and N. D. Kushuh, Solid State Commun. **89**, 575 (1994).

[9] N. Hanasaki, S. Kagoshima, N. Miura, and G. Saito, J. Phys. Soc. Jpn. **65**, 1010 (1996).

[10] P. Foury-Leylekian, S. Ravy, J.-P. Pouget, and H. Müller, Synth. Met. **137**, 1271 (2003).

[11] J. S. Brooks, C. C. Agosta, S. J. Klepper, M. Tokumoto, N. Kinoshita, H. Anzai, S. Uji, H. Aoki, A. S. Perel, G. J. Athas *et al.*, Phys. Rev. B **52**, 14457 (1995).

[12] D. Andres, M. V. Kartsovnik, W. Biberacher, K. Neumaier, E. Schuberth, and H. Müller, Phys. Rev. B **72**, 174513 (2005).

[13] H. Mori, S. Tanaka, M. Oshima, G. Saito, T. Mori, Y. Maruyama, and H. Inokuchi, Bull. Chem. Soc. Jpn. **63**, 2183 (1990).

[14] N. Harrison, E. Rzepniewski, J. Singleton, P. J. Gee, M. M. Honold, P. Day, and M. Kurmoo, J. Phys.: Condens. Matter **11**, 7227 (1999).

[15] Y. Iye, M. Baxendale, and V. Z. Mordkovich, J. Phys. Soc. Jpn. **63**, 1643 (1994).

[16] J. Caulfield, J. Singleton, P. T. J. Hendriks, J. A. A. J. Perenboom, F. L. Pratt, M. Doporto, W. Hayes, M. Kurmoo, and P. Day, J. Phys.: Condens. Matter **6**, L155 (1994).

[17] K. Uchida, R. Yamaguchi, T. Konoike, T. Osada, and W. Kang, J. Phys. Soc. Jpn. **82**, 043714 (2013).

[18] J. Caulfield, S. J. Blundell, M. S. L. du Croo de Jongh, P. T. J. Hendriks, J. Singleton, M. Doporto, F. L. Pratt, A. House, J. A. A. J. Preneboom, W. Hayes *et al.*, Phys. Rev. B **51**, 8325 (1995).

[19] N. Harrison, J. Caulfield, J. Singleton, P. H. P. Reinders, F. Herlach, W. Hayes, M. Kurmoo, and P. Day, J. Phys.: Condens. Matter **8**, 5415 (1996).

[20] W. Kang, T. Osada, Y. J. Jo, and H. Kang, Phys. Rev. Lett. **99**, 017002 (2007).

[21] W. Kang, Y. J. Jo, D. Y. Noh, K. I. Son, and O.-H. Chung, Phys. Rev. B **80**, 155102 (2009).

[22] M. V. Kartsovnik, H. Ito, H. Mori, T. Mori, G. Saito, and S. Tanaka, J. Phys.: Condens. Matter **6**, L479 (1994).

[23] K. Murata, H. Yoshino, H. O. Yadav, Y. Honda, and N. Shirakawa, Rev. Sci. Instrum. **68**, 2490 (1997).

[24] L. D. Jennings and C. A. Swenson, Phys. Rev. **112**, 31 (1958).

[25] N. Hanasaki, S. Kagoshima, N. Miura, and G. Saito, Phys. Rev. B **63**, 245116 (2001).

[26] M. V. Kartsovnik, P. A. Kononovich, V. N. Laukhin, and I. F. Schegolev, Pis'ma Zh. Eksp. Teor. Fiz. **48**, 498 (1988) [JETP Lett. **48**, 541 (1988)].

[27] K. Kajita, Y. Nishio, T. Takahashi, W. Sasaki, R. Kato, and H. Kobayashi, Solid State Commun. **70**, 1189 (1989).

[28] K. Yamaji, J. Phys. Soc. Jpn. **58**, 1520 (1989).

[29] A. G. Lebed, Pis'ma Zh. Eksp. Teor. Fiz. **43**, 137 (1986) [JETP Lett. **43**, 174 (1986)].

[30] T. Osada, A. Kawasumi, S. Kagoshima, N. Miura, and G. Saito, Phys. Rev. Lett. **66**, 1525 (1991).

[31] M. J. Naughton, O. H. Chung, M. Chaparala, X. Bu, and P. Coppens, Phys. Rev. Lett. **67**, 3712 (1991).

[32] G. M. Danner, W. Kang, and P. M. Chaikin, Phys. Rev. Lett. **72**, 3714 (1994).

[33] H. Yoshino, K. Saito, K. Kikuchi, H. Nishikawa, K. Kobayashi, and I. Ikemoto, J. Phys. Soc. Jpn. **64**, 2307 (1995).

[34]T. Osada, S. Kagoshima, and N. Miura, Phys. Rev. Lett. **77**, 5261 (1996).

[35]M. V. Kartsovnik, D. Andres, S. V. Simonov, W. Biberacher, I. Sheikin, N. D. Kushch, and H. Muller, Phys. Rev. Lett. **96**, 166601 (2006).

[36]J. S. Brooks, C. C. Agosta, S. J. Klepper, M. Tokumoto, N. Kinoshita, H. Anzai, S. Uji, H. Aoki, A. S. Perel, G. J. Athas *et al.*, Phys. Rev. Lett. **69**, 156 (1992).

[37]T. Kouno, T. Osada, M. Hasumi, S. Kagoshima, N. Miura, M. Oshima, H. Mori, T. Nakamura, and G. Saito, Synth. Met. **55–57**, 2425 (1993).

[38]M. V. Kartsovnik, A. V. Kovalev, and N. D. Kushch, J. Phys. I **3**, 1187 (1993).

[39]D. Andres, M. V. Kartsovnik, W. Biberacher, H. Weiss, E. Balthes, H. Müller, and N. Kushch, Phys. Rev. B **64**, 161104 (2001).